Modelling radiative-shocks created by laser-cluster interactions

Contact: robbie.scott@stfc.ac.uk

R.H.H. Scott, N. Booth, S.J. Hawkes, D. Symes
Central Laser Facility,
STFC Rutherford Appleton Laboratory,
Harwell Oxford, OX11 0QX,
United Kingdom

H.W. Doyle
Clarendon Laboratory
University of Oxford
Oxford, OX1 3PU, United Kingdom

S.I. Olsson-Robbie, H.F. Lowe, C. Price, D. Bigourd, S. Patankar, K. Mecseki, R.A. Smith
Department of Physics, The Blackett Laboratory,
Imperial College London,
SW7 2AZ, United Kingdom

J. Fyrth, E.T. Gumbrell
Plasma Physics Division
AWE Aldermaston
Reading, RG7 4PR,
United Kingdom

Abstract

Radiative-shocks induced by laser-cluster interaction are modelled numerically using radiation-hydrodynamics. A good agreement is obtained between experiment and simulations, indicating that non-LTE effects are clearly important in the experimental regime examined, particularly at early-times due to the elevated temperatures and low densities. A range of issues associated with the successful modelling of such scenarios are identified and discussed, including the effects of the various atomic models used to generate the opacity data (LTE/steady state non-LTE/collisional-radiative non-LTE), and their effects on the shock generation and propagation. In going from LTE, to steady state non-LTE and finally to time dependent non-LTE, the simulated shocks are systematically reduced in amplitude, increased in width and reduced in propagation velocity while the amplitude of the radiative precursor is increased. This trend is broadly consistent with the the plasma being increasingly emissive with the more sophisticated and accurate non-LTE atomic models. Finally, it is found that the shock trajectory is a degenerate measure of the initial plasma conditions.

1 Introduction

Laboratory experiments of relevance to astrophysics are valid because the mathematical models governing radiation-hydrodynamics are invariant under the appropriate transformation and hence can be rescaled between laboratory and astrophysical systems [1]. Today's laser systems allow the generation of plasmas which are in regimes of relevance to certain scaled astrophysical systems.

Shock waves are particularly interesting astrophysical systems as they are ubiquitous throughout the universe and play a crucial role in the transport of energy into the interstellar medium [2] and the generation of high-energy cosmic-rays [3, 4]. In the limit of a weak shock, the role of radiation in the shock's energy balance is small and the pressure, density and temperature profiles across the shock have the classical step-like character. However as the shock strength, and hence downstream temperature increases, the radiation flux from the shock's front surface increases rapidly (as σT^4, where σ is the Stephan-Boltzmann constant, and T the electron temperature). The emitted radiation is absorbed by the upstream material over a distance of the order of the photon mean-free-path. The absorption of the photon heats the upstream material, creating a 'shelf' or precursor in temperature, density and pressure which precedes the shock front. Importantly the photon absorption may also cause electron excitation and ionisation of the upstream media, this in turn modifies the local emissivity and opacity creating a complex system where radiation transport plays a crucial role in the energy balance of the system as a whole. Consequently the free electron density level may be elevated upstream of the shock (a radiative pre-cursor), providing a clear experimental observable that the shock is radiating on an energetically significant level. Such systems are called radiative-shocks, they have been observed around a wide variety of astronomical objects e.g. accretion shocks, pulsating stars, supernovae in their radiative cooling stage, bow shocks of stellar jets in the galactic medium, collisions of interstellar clouds, entry of rockets or comets into planetary atmospheres, and in the late-time disassembly of unignited inertial confinement fusion capsules [5].

Atomic clusters are created in the laboratory by the rapid adiabatic expansion of a gaseous element into a vacuum. The rapid drop in temperature condenses the gas into clusters of size $\sim 10-100\,nm$. On a microscopic scale, the clusters are over-dense to optical laser light, while the cluster 'gas' is macroscopically under-dense. The laser energy is absorbed locally to the over-dense clusters. Due to the spherical structure of the clusters,

the laser's electric field excites a resonantly driven oscillation of the (partially ionised) cluster's electrons[6]. This resonance occurs when the light frequency is near to the cluster's plasma frequency, and causes an associated resonance in the optical absorption spectrum.

Laser-cluster experiments e.g. [7, 8, 9] and references therein, report high laser absorption fractions into thin filaments of width of the order of the laser focal spot size. The generation of a thin, hot filament of plasma in turn creates a cylindrical blast-wave[10], where a sudden release of energy from a region of small spatial extent causes an expanding shock to sweep up material ahead of the shock. By increasing the material atomic number Z, and hence Z^* (the ionisation state), the radiative properties of the shock can be controlled for a given shock temperature.

When a plasma is at Thermodynamic Equilibrium, the whole system, comprised of electrons, atoms, ions and radiation can be fully described by statistical mechanics, with each of the particle distributions characterised by the same characteristic temperature T. The Electron Energy Distribution Functions (EEDF) is a Maxwellian of temperature T, while the relative populations of the excited states, the Atomic State Distribution Function (ASDF) are populated in Saha-Boltzmann equilibrium at the temperature and density concerned, and the radiation field is described by the Planck function at T. Under Thermodynamic Equilibrium each electron state transition process is balanced by its inverse process and the systems is said to be in *detailed balance*. However this is rarely true, since the plasma must be sufficiently large such that the optical depth is very large for all emitted radiation frequencies at all points in the plasma in order for equilibrium to be established.

Gradients in space and/or time can cause photons to escape from the plasma, this in turn causes the radiative energy distribution function to deviate from the Planck function, affecting the detailed balance of electrons, ions and atoms. In principal the system is no longer in Thermodynamic Equilbrium, if however the energy lost due to radiation is relatively small compared to the overall energy balance, the Saha-Boltzmann and Maxwellian distributions are still valid and the system is said to be in Local Thermodynamic Equilibrium (LTE), in which case $T_{ASDF} = T_e = T_i \neq T_r$, where T_{ASDF} is the temperature characterising the excited states and T_e, T_i and T_r are the electron, ion and radiation temperatures respectively. A further departure from TE occurs when $T_e \neq T_i$, in such systems $T_{ASDF} \sim T_e$.

As a general rule, a plasma is said to *not* be in equilibrium if the rate of photon absorptions $\gg$ rate of electron collisions. The commonly used McWhirter Criterion [11] indicates that the ratio of the rate of electron collisions to the rate of photon absorptions should be at least 10. This can be expressed by the relation [12]: $n_e(cm^3) > 1.6 \times 10^{12} T^{1/2} \Delta E^3_{nm}$ where n_e is the electron number density T in K and E_{nm} is the largest energy gap between adjacent levels in eV. However as discussed in a comprehensive recent work by Cristoforetti *et al.* [12] this criterion can only rigorously be applied in a stationary, homogeneous plasma which is optically thin. For these circumstances if this criterion is *not* fulfilled, LTE *cannot* be true, importantly however even then it only indicates when LTE *may* be true, rather than when LTE *is* true. Nevertheless a system is more likely to be in LTE if the density is high and the temperature low.

In the case of time-dependent and inhomogeneous plasmas, two further criterion should be verified [12]. Firstly to account for the transient nature of the plasma, the temporal variation of thermodynamic parameters should be small over the excitation and ionisation equilibration timescales. Secondly the scale length of variations in electron temperature and number density in the plasma should be larger than the particle diffusion lengthscales over the time it takes for the plasma to relax to equilibrium. When spatial and/or temporal gradients are strong or when radiative processes significantly affect the overall energy balance, the system still further departs from Thermodynamic Equlibrium, usually requiring a space and time resolved Collisional-Radiative (CR) model[13] to obtain a solution. Here all of the various radiative and collisional processes (and their inverses) that take place between electrons, ions and photons must be considered. In order to calculate the populations of the numerous energy levels a large number of coupled rate equations are solved, requiring an iterative approach. This must be solved simultaneously with the radiative transfer equation. For higher Z elements this can be an extremely challenging calculation given the huge numbers of energy levels, transitions, cross-sections etc involved.

2 Simulations

Modelling the generation and subsequent propagation of radiative-shocks generated by laser-cluster interactions is extremely challenging due to the disparate spatial and temporal scales of the various aspects of the interaction: the clusters sizes are $\leq 100\,nm$ while the shock propagates over $\sim 1\,cm$, the laser duration is $30\,fs$ while that of the shock is $\sim 100\,ns$. The complex kinetics associated with high-intensity laser-cluster interactions would be captured by particle-in-cell (PIC) simulations, however due to the computation overheads of PIC techniques, it would not be feasible to run to the tens of nano-second timescales of the experimentally measured radiative-shock propagation and evolution. Furthermore due to the relatively simple ionisation

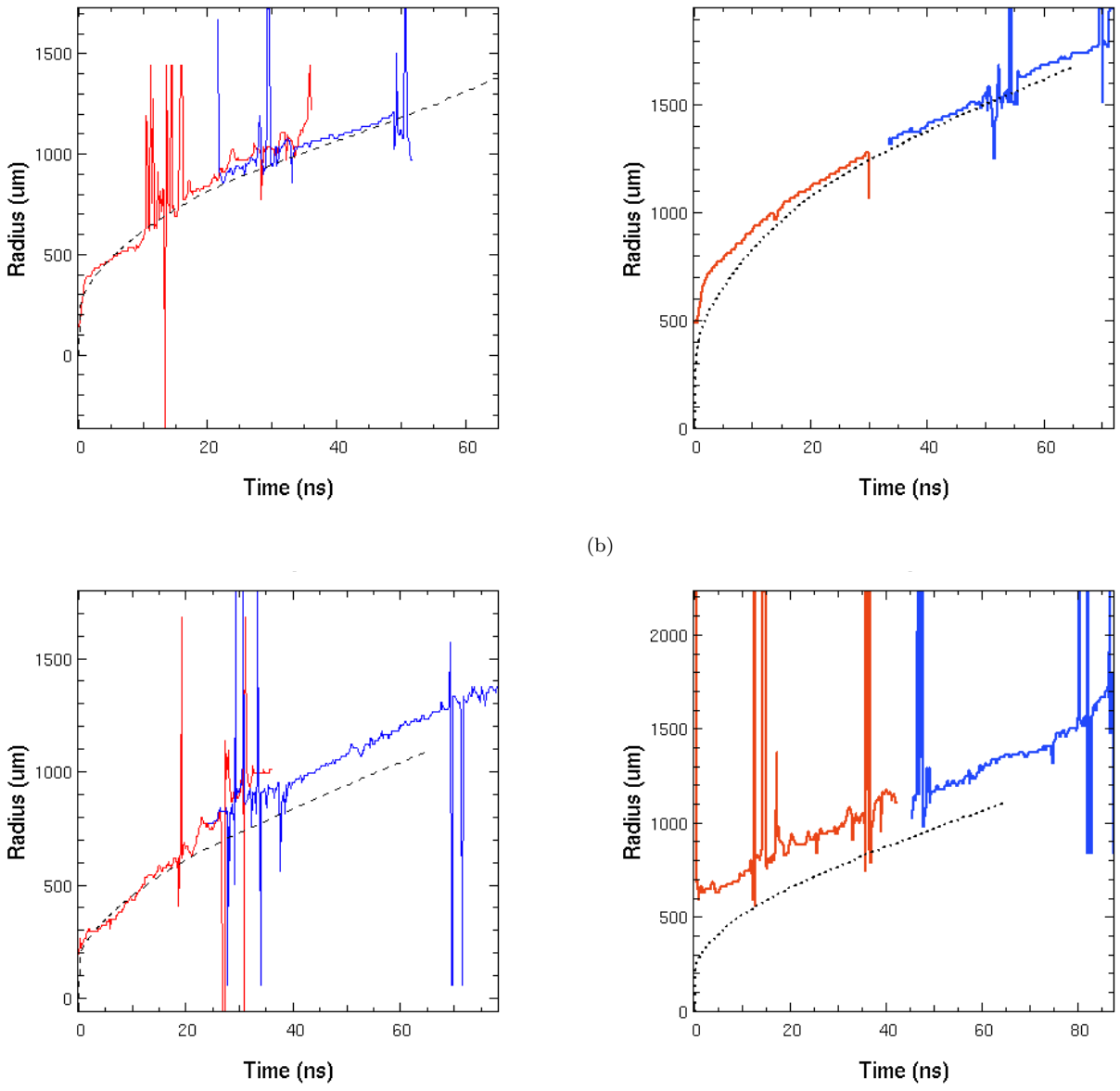

Figure 1: Plots of early and late time experimental data (red and blue lines respectively), with radiation-hydrodynamic simulations over plotted in black. (a) is the 'tuned' Krypton baseline run, all other simulations use the initial conditions from (a) scaled appropriately to reflect the changes in experimental conditions. (b) Krypton with density scaled from run (a), (c) Krypton with energy scaled from run (a) , (d) Xenon run with scaled density from run (a).

models employed even by cutting edge PIC modelling, this technique is unlikely to capture anything other than the most simple atomic kinetics and certainly not the effects of detailed opacity and re-emitted radiation. As the principal aim of this modelling was to attempt to reproduce and better understand the experimental observations, a pragmatic but less rigorous approach was adopted by ignoring kinetic effects and instead performing radiation-hydrodynamics modelling with initial conditions based upon the experimental observations.

One dimensional radiation-hydrodynamics simulations were performed in cylindrical geometry using the radiation-hydrodynamics codes Hydra [14], Helios [15] and Hyades[16]. The problem was initialised with uniform gas density throughout. The region where the laser deposited its energy was represented by a hot region with a radially varying temperature profile, Gaussian in form.

Conceptually this corresponds to the experimentally observed filament. The initial gas density, filament radius and total filament energy, were first set to correspond with those observed experimentally. The plasma was initialised with a Gaussian radial variation in ion and/or electron temperature (depending on the particular run), peaked on axis. In order to ensure approximate energetic consistency with the experiment, the integral of the filament internal energy (dictated by initial density, filament radius, species and temperature distribution) over the filament volume equalled the product of the laser energy with the measured absorption fraction. Hydra, Helios and Hyades simulations were run with multi-group radiation diffusion, the equations of state were QEOS, Propaceous or SESAME respectively, while numerous opacity options were utilised: Local Thermodynamic Equilibrium (LTE), non-LTE optically thin, and non-LTE collisional-radiative(CR) modelling. For the non-LTE CR modelling a variety of atomic models were used, from the most basic where all shells were collapsed into the principal quantum number to more sophisticated 'Detailed Configuration Accounting' type models where energy level splitting by angular quantum number is included. Both time dependent and steady state non-LTE treatments were evaluated, in the steady state approximation no iteration of the various rate equations is performed hence *detailed balance* - where the rates of each of the transitions is balanced by its inverse - is not obtained.

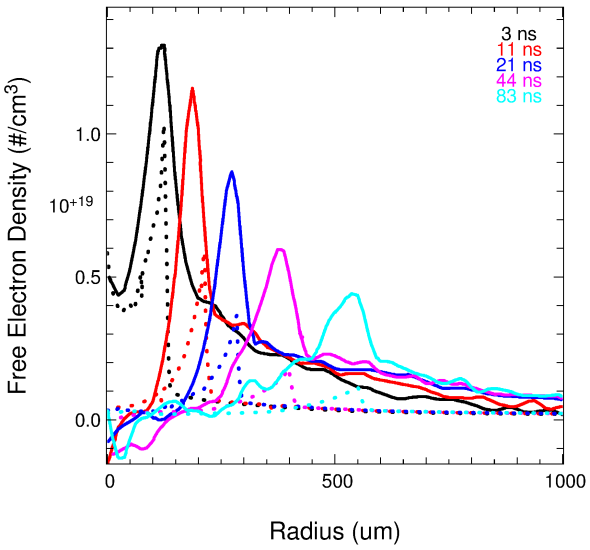

Figure 2: Hyades steady state non-LTE simulation data (dashed lines) over-plotted on the experimental data (solid lines). In this simulation, which uses the nominal experimental density, the radiative pre-cursor amplitude is under-predicted.

3 LTE modelling of Astra-Gemini Radiative-Shock Experiment

This experiment was performed on the Astra-Gemini laser at the Central Laser Facility of the STFC Rutherford Appleton Laboratory. $15\,J$ of $800\,nm$ laser light was focussed to $\sim 15\,\mu m$ FWHM in a pulse of duration $30\,fs$, yielding a peak intensity of $5 \times 10^{20}\,Wcm^{-2}$. Argon, Krypton and Xenon clusters were created by expansion of the gases through a nozzle on entry to the interaction chamber. The laser was focussed above the nozzle and approximately at its front edge.

Time integrated imaging of the second harmonic of the laser light showed the relative uniformity of the laser energy deposition along a filament of length $\sim 3\,mm$. The principal shock measurement diagnostic was streaked Schlerien which imaged both fronts of the shock expansion as a function of time at a particular location along the filament length. As the heated filament of plasma was relatively long in comparison to the radial propagation distance, the shock was approximately cylindrically symmetric over a large central region. The Schlerien measurements were made within this central region.

The simulations described in this section were performed using Hydra with LTE opacities, the runs were initialised with the measured or inferred experimental values. These values were: density (measured offline), laser energy (measured), laser absorption (measured) and filament radius (inferred from the shock trajectory). It was found that in order to match the experimental shock trajectory, the filament radius and internal energy were consistent with the experimental values, however the density in the simulation had to be significantly higher ($\sim 10\times$) than that subsequently measured offline. It is most likely that the necessity for a high background gas density is due to the use of LTE opacities, which increases the shock velocities in comparison to more sophisticated non-LTE atomic models. This is discussed in more detail in section 4.

The experimental data is comprised of shot pairs, these shots have the same experimental parameters within the margin of reproducibility but have experimental measurements over differing spatio-temporal ranges to enable the full shock trajectory to be reconstructed. Figure 1(a) shows a shot pair in Krypton plotted against the corresponding LTE simulation. The 'tuned' initial conditions for Krypton were used as a baseline for subsequent runs. These experiments also used Krypton but at differing initial densities - for the matching simulations only the ratios of the densities were altered, in direct accordance with the experimental parameters. These are shown in figure 1(b). It can be seen that the shock trajectory of the

simulation remains in reasonable agreement with the experiment. A similar exercise is shown in figure 1(c), here only the filament internal energy has been altered with respect to figure 1(a), again to directly reproduce the change in experimental conditions. Again, the simulation matches the experiment reasonably well, with the early time radius and velocity and late time velocity being a good reproduction of the trajectory, although the late-time radius is somewhat small.

Using a similar simulation methodology to the above a shot pair using Xenon clusters was simulated. Here only the initial density and material was altered in comparison to the Krypton baseline. This is shown in figure 1(d). Here the simulated shock velocity is accurate, however the radius is small in comparison to the experiment throughout. The increased discrepancy observed here with Xenon - a higher Z material - is most likely due to the increased importance of radiative effects due to associated increases in Z^* and hence bremsstrahlung rates combined with the relative lack of sophistication of the atomic models employed for this simulation.

4 Non-LTE modelling of Radiative-Shock Experiments

This section deals with the application of non-LTE radiation hydrodynamic modelling techniques to a dataset obtained during a separate experimental campaign. This experiment is described in detail by Osterhoff *et al.* in [9]. Briefly, the experimental characteristics were as follows: an $f/7$ spherical mirror focused into plume of Xenon clusters with an intensity of up to $1 \times 10^{18}\, W cm^2$, creating a hot plasma filament approximately $65\,\mu m$ in diameter and $4\,mm$ long which developed into a strong cylindrical blast wave. Xenon clusters were irradiated at two different average gas densities: $2.5 \times 10^{-4}\, gcm^{-3}$ with $360\,mJ$ pulse energy and $1.6 \times 10^{-4}\, gcm^{-3}$ with $440\,mJ$ per pulse, although only the latter is dealt with here. Time resolved interferometry was the principal diagnostic, giving an absolute measure of the free electron density at various discrete times.

The solid lines in figure 2 depict the interferometrically inferred experimental free electron density at various times. Upstream of the shock front (to the right), the free electron density is raised significantly above the background density (initial ion density is $7.3 \times 10^{17}\, ions/cm^3$), this is caused by ionisation of the upstream material by photons emitted from the shock front. Accurate modelling of this system is challenging as it is highly constrained by the experimental initial conditions and observations - the bulk energetics are constrained by the shock radius and velocity, while the details of the ionisation and associated radiation

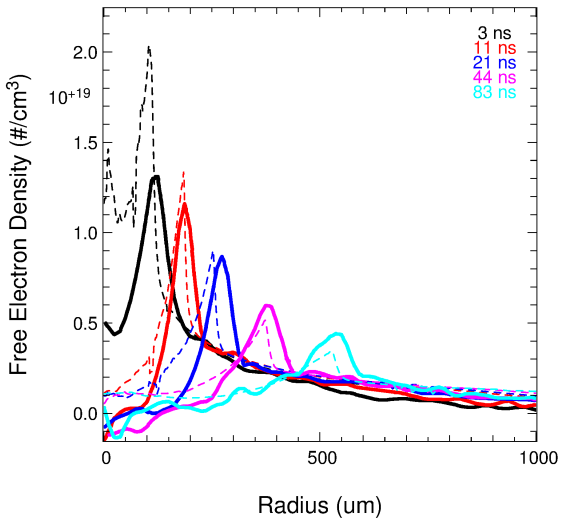

(a)

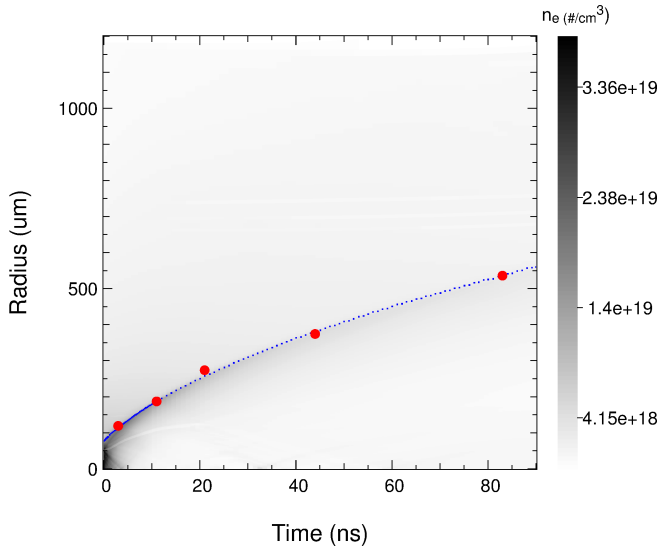

(b)

Figure 4: (a) Hyades simulation data (dashed lines) over plotted on the experimental data (solid lines). (b) shows the simulated shock trajectory (blue points) overplotted on the experimental shock trajectory (red points). This simulation was performed using the time dependent non-LTE model with a LTE transition temperature of $35\,eV$. Despite the peak simulated electron density at $3\,ns$ exceeding the experimental data, this was the best fit obtained.

transport dictate the radiation emission and structure of the radiative pre-cursor, which in turn feedback into the shock profile and strength. The presence of the radiative pre-cursor provides a clear indication that the upstream plasma is not completely optically thin to the radiation emitted by the shock and/or downstream

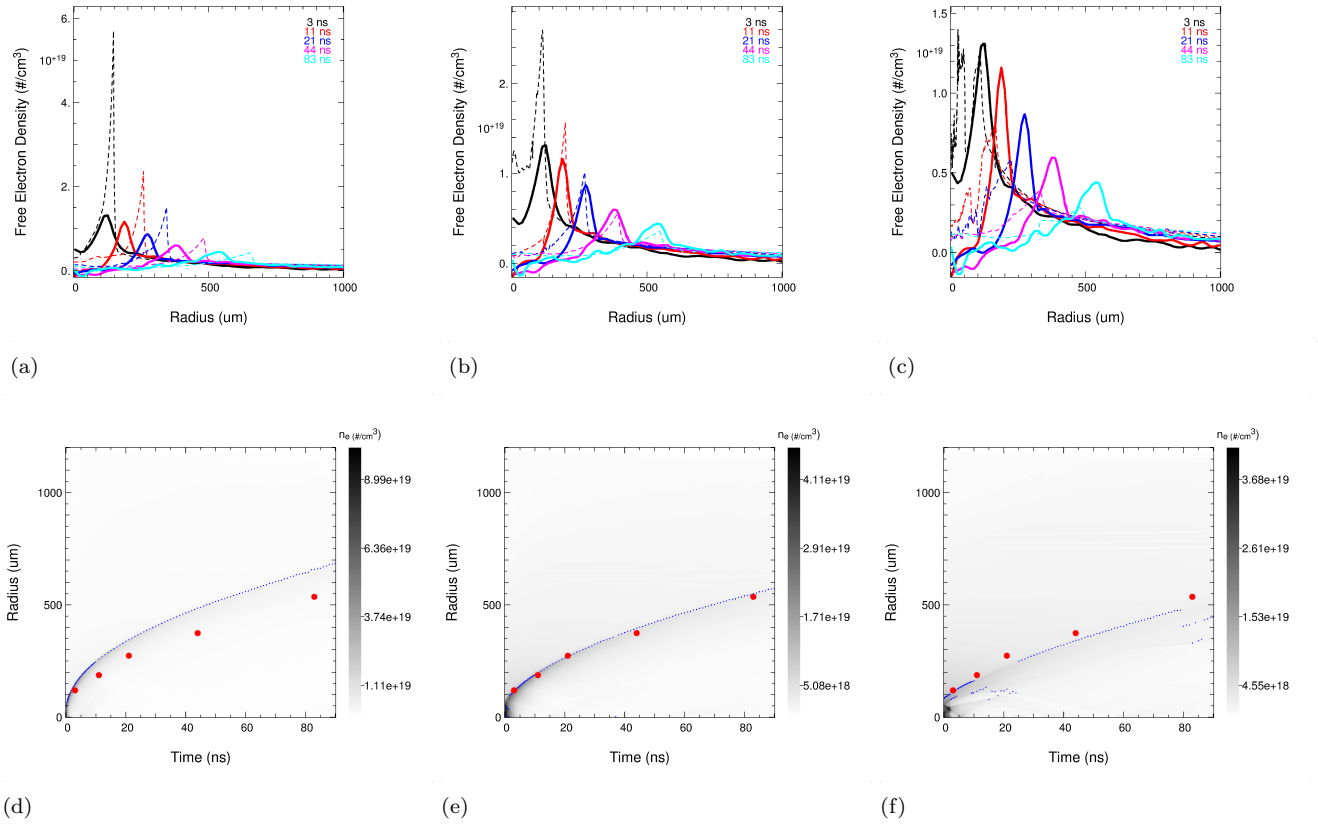

Figure 3: Top row (figures (a)-(c)) shows Hyades simulation data (dashed lines) over plotted on the experimental data (solid lines). Bottom row (figures (d)-(f)) shows the simulated shock trajectory (blue points) overplotted on the experimental shock trajectory (red points). Simulations in the left column (figs. (a) & (d)) use LTE opacities, the central column (figs. (b) & (b)) use a steady state non-LTE atomic model to generate the opacities, while the right column (figs. (c) & (f)) uses a time dependent non-LTE atomic model to generate the opacity data. The steady state non-LTE simulation was tuned to best match the data by changing the internal energy initially deposited in the electrons. The LTE and time dependent non-LTE runs used exactly the same initial conditions as the steady state non-LTE simulation. It can be seen that in going from LTE, to steady state non-LTE and finally to time dependent non-LTE, the simulated shocks are systematically reduced in amplitude, increased in width and propagate more slowly.

material, as it is the coupling of this radiation which heats the material upstream of the main shock front, locally raising the ionisation level and hence the free electron density, this is visible as the pre-cursor.

In order to reproduce the experimental data an extensive search of the experimental parameter space was performed using both Helios and Hyades with their differing equations of state and opacity/atomic models. Parameter space searches included variations in initial density, filament radius and internal energy, variations from the experimental values were confined to approximately a factor of two. The Helios runs were initialised by distributing the internal energy with a radial Gaussian form within both the ion and electron populations via the species temperatures, which were equal at a given radius. In the Hyades runs the internal energy was also deposited solely within the electron population, in order to attempt to more accurately reflect the laser energy deposition into the electrons. Radiation transport was modelled using the diffusive approximation. A range of atomic kinetics/opacity models were employed: LTE, steady-state non-LTE, and time-dependent non-LTE (full Collisional-Radiative). Varying degrees of sophistication of atomic model were also used, these included hydrogenic models, hydrogenic models with term splitting (Detailed Configuration Accounting), and Unresolved Transition Array schemes. The equations of state used were Propaceous (Helios) and SESAME (Hyades). The results of the two codes were qualitatively similar, showing similar differences when switching between LTE, steady-state non-LTE, and time-dependent non-LTE. The detailed discussions below refer to the modelling performed with Hyades.

A close, but not exact, match of both the measured

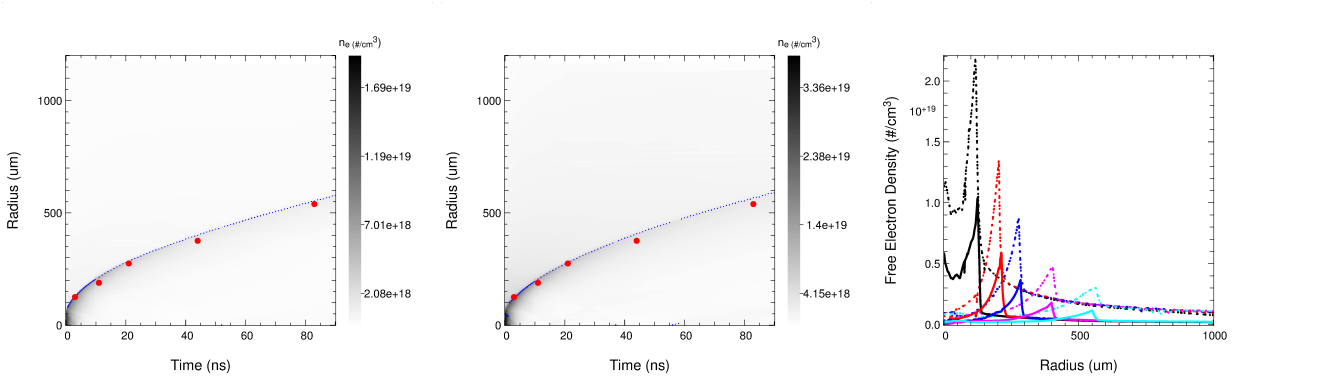

(a) (b) (c)

Figure 5: (a) and (b) show steady state non-LTE Hyades simulations overlaid on the experimental shock trajectory (red points). Both simulations have almost identical shock trajectories but the initial conditions which generated these trajectories were quite different: (a) has internal energy $0.33\,J$, density $4.1\,gcm^{-3}$, while (b) has an internal energy of $0.1\,J$ and density of $1.6\,gcm^{-3}$). (c) shows the associated electron density profiles at various times, the dotted lines are from the simulation shown in (a), while the solid lines correspond to the simulation shown in (b).

free electron density profiles and the shock trajectory was obtained. In order to best match the data, the initial density was set to that of the experiment, the filament radius to $50\mu m$ full-width-at-half-maximum (approximately the experimental laser focal spot size) while the internal energy initially deposited in the electrons was tuned by changing the ion and/or electron temperature. LTE, steady-state non-LTE, and time-dependent non-LTE (CR) atomic models were used in order to find a best match to the data. When using the experimental background density and a peak electron temperature of $400\,eV$ (internal energy $0.11\,J$) the principal discrepancy between simulation and experiment is in the width of the peak and the amplitude of the radiative precursor, as shown in fig. 2. Assuming all of the laser energy went into internal energy, and was not lost to e.g. Coulomb explosion of the clusters, this implies a relatively small absorption fraction of $\sim 25\%$ in comparison to experimental data. In order to increase the coupling of the radiation emitted by the shock to the upstream material, the initial background gas density was artificially increased to $5 \times 10^{-4}\,gcm^{-3}$ ($3.1\times$ the experimentally measured value). Due to the increase in density, the filament internal energy was $0.3\,J$ in this simulation, at 68% this compares favourably with the $> 50\%$ laser absorption routinely reported in cluster experiments. The steady-state non-LTE modelling obtained using these parameters is shown in figures 3(b) and (e).

It was found that the non-LTE models gave the best match to the data. The CR equivalent to 3(b) and (e) is shown in (c) and (f), no attempt has been made to independently tune the CR run. The full CR model appears to capture the early time dynamics better - the shock amplitude and width closely resembles the experiment - although it over predicts the amplitude of the peak on axis, while at later times the steady-state NLTE model is better. In a detailed analysis of the data from the same experiment, Rodriguez *et al.* [2] indicate that the switch to NLTE conditions occurs above $12\,eV$ for the density in these simulations. One interpretation of the CR simulations, which use the $12\,eV$ LTE to NLTE transition temperature, is that the NLTE model is over predicting the plasma emissivity at late times (the simulated plasma temperature is above $12\,eV$ until $\sim 30\,ns$) and hence under estimating the shock amplitude. By increasing the transition temperature to $35\,eV$ it was possible to obtain a better match to the the late time data, as shown in figure 4. It should be noted that the necessity to use an elevated LTE to NLTE transition temperature does *not* mean that the transition temperature quoted by Rodriguez *et al* is incorrect, merely that this value gives a better match to data in the necessarily simplified atomic models employed in radiation-hydrodynamic modelling. Although the peak amplitude at $3\,ns$ was slightly higher than that obtained experimentally. Part of the observed discrepancy in the peak amplitude may be explained by the experimental spatial resolution, which was approximately $125\,\mu m/pixel$. This would also bring the early time steady-state NLTE towards the experimental data.

5 Discussion

The best match obtained with the steady-state NLTE model is shown in figure 3 (b) and (e). Using identical initial conditions, this run was repeated with LTE opacities (figures 3 (a) and (d)) and the full CR model (3 (c) and (f)) in order to evaluate the effects of the various opacity models. Comparing the three runs

reveals a trend; in going from LTE, to steady state non-LTE and finally to time dependent non-LTE, the simulated shocks are systematically reduced in amplitude, increased in width and reduced in propagation velocity while the amplitude of the radiative precursor is increased. This trend is broadly consistent with the the plasma being increasingly emissive with the more sophisticated and accurate non-LTE atomic models.

The experimental shock trajectory was reproducible with relative ease in comparison to the more restrictive electron density profiles. This was possible with the LTE, steady state non-LTE and time dependent non-LTE models although the initial conditions required to create the shock trajectory differed significantly. Furthermore even with a given simulation opacity/atomic model setup, it was possible to reproduce the shock trajectory with a range of density/internal energy initial conditions, illustrating that the shock trajectory is a degenerate measure of the initial conditions. This is illustrated in figure 5 which shows two simulations, both of which approximately match the experimental shock trajectory (fig. 5 (a) & (b)), while the electron density profiles fig. 5 (c) are quite different.

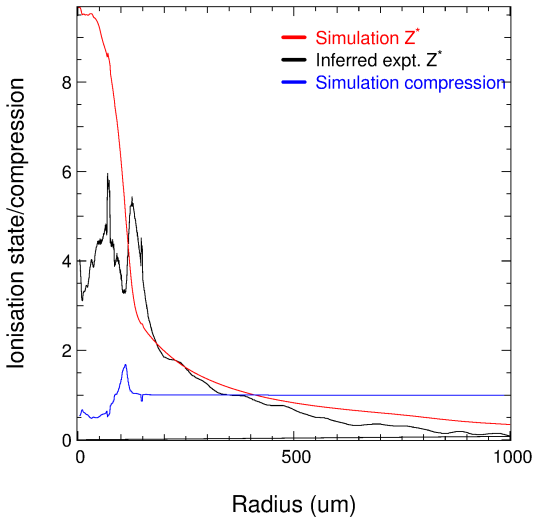

Figure 6: Ionisation states at $3\,ns$. Red line is hyades, black line is the inferred experimental value using the ion density from the simulation at $3\,ns$ (compression in blue).

The radiation-hydrodynamic simulations used to model this experiment ignore the detailed kinetics of the laser-cluster interaction, but not those of the atomic physics, assuming instead a heated filament with a Gaussian profile. Although these initial conditions are clearly an approximation, it was found that the radiation-hydrodynamics were relatively insensitive to changes in the initial conditions, leading to the tentative conclusion that after the initial laser-cluster interaction, (non-atomic) kinetics play a relatively unimportant role in the subsequent shock formation and propagation. Modelling the early time kinetics will be the subject of a future publication.

The initial gas consists of atomic clusters, not a uniform gas, as assumed in the radiation-hydrodynamics simulations. Due to the local extreme variations in density it is likely that the transport of radiation through a cluster gas is quite different to that through a homogeneous plasma of equal macroscopic density (to the spatially averaged cluster gas density) and temperature. Accurately modelling radiation transport in such a medium would require an extremely high spatial resolution multi-dimensional simulation, and may even require Implicit Monte Carlo radiation transport due to the local inhomogeneities. At early times clusters will exist, however by $3\,ns$ (the time of the first experimental electron density lineout) the data suggests they may have been destroyed - even on the edge of the experimental field of view a plasma exists with $Z^* \sim 1$. The simulations show that, the central filament rapidly radiates, expands and consequently cools - in the first $0.1\,ns$ the electron temperature reduces from $\sim 500\,eV$ to $\sim 50\,eV$. Consequently it is likely that this ionisation state would have to be induced by radiation emitted at very early times, before this cooling occurs. The energy absorption required to create such ionisation states imply that the clusters will have been destroyed by hydrodynamic expansion and hence a relatively uniform plasma will have formed before significant shock propagation occurs. This leads us to the conclusion that using a homogeneous gas as the initial conditions for the hydrodynamics is most probably adequate.

The total energy required to induce the experimentally observed ionisation levels at $3\,ns$ can be approximated using the associated experimental electron density data. The ion density (n_i is taken from the best fitting steady state non-LTE simulation. Z^* was calculated at the earliest experimental time ($3\,ns$) using $Z^*(r) = n_e(r)/n_i$, where r is the plasma radius. Assuming a cylindrical plasma of length $4\,mm$ (as per experiment), the lineout was discretised onto a mesh enabling the calculation of the volume and hence the ion number as a function of radius. The required total ionisation energy is hence $E_{ionise}(r) = Z^*(r).E_{ipot}(Z^*).n_{iBg}$ where $E_{ipot}(Z^*)$ is a fit to the cumulative ionisation energy states as a function of Z^* for Xenon [17]. Integrating this over the plasma volume yields a total energy required to create the observed ionisation states of $0.02\,J \sim 5\%$ of the laser energy. The calculated ionisation states are shown in figure 6.

6 Conclusion

Radiative-shocks induced by laser-cluster interactions are an extremely challenging experimental scenario to model numerically due to their disparate spatio-temporal scales, complex early-time kinetics, high electron temperatures and low density. The radiation-hydrodynamic modelling performed indicates that non-LTE effects are clearly important in the experimental regime examined, particularly at early-times due to the elevated temperatures and low densities. A range of issues associated with the successful modelling of such scenarios have been identified and discussed, including the effects of the various atomic models used to generate the opacity data (LTE/steady state non-LTE/collisional-radiative non-LTE). In going from LTE, to steady state non-LTE and finally to time dependent non-LTE, the simulated shocks are systematically reduced in amplitude, increased in width and reduced in propagation velocity while the amplitude of the radiative precursor is increased. This trend is broadly consistent with the the plasma being increasingly emissive with the more sophisticated and accurate non-LTE atomic models. Finally, it was shown that the induced shock trajectory is degenerate with relation to the plasma initial conditions.

Acknowledgements

We gratefully acknowledge supporting funding from EPSRC grant EP/G001324/1 and EPSRC doctoral training account and AWE Aldermaston Industrial CASE Studentships.

References

[1] S. Bouquet, E. Falize, C. Michaut, C.D. Gregory, B. Loupias, T. Vinci, and M. Koenig. From lasers to the universe: Scaling laws in laboratory astrophysics. *High Energy Density Physics*, 6(4):368 – 380, 2010.

[2] R. Rodriguez, G. Espinosa, J.M. Gil, R. Florido, J.G. Rubiano, M.A. Mendoza, P. Martel, E. Minguez, D.R. Symes, M. Hohenberger, and R.A. Smith. Analysis of microscopic magnitudes of radiative blast waves launched in xenon clusters with collisional-radiative steady-state simulations. *Journal of Quantitative Spectroscopy and Radiative Transfer*, 125(0):69 – 83, 2013.

[3] A. R. Bell. The acceleration of cosmic rays in shock fronts – i. *Monthly Notices of the Royal Astronomical Society*, 182(2):147–156, 1978.

[4] A. R. Bell. Turbulent amplification of magnetic field and diffusive shock acceleration of cosmic rays. *Monthly Notices of the Royal Astronomical Society*, 353(2):550–558, 2004.

[5] A. Pak, L. Divol, G. Gregori, S. Weber, J. Atherton, R. Bennedetti, D. K. Bradley, D. Callahan, D. T. Casey, E. Dewald, T. Doppner, M. J. Edwards, J. A. Frenje, S. Glenn, G. P. Grim, D. Hicks, W. W. Hsing, N. Izumi, O. S. Jones, M. G. Johnson, S. F. Khan, J. D. Kilkenny, J. L. Kline, G. A. Kyrala, J. Lindl, O. L. Landen, S. Le Pape, T. Ma, A. MacPhee, B. J. MacGowan, A. J. MacKinnon, L. Masse, N. B. Meezan, J. D. Moody, R. E. Olson, J. E. Ralph, H. F. Robey, H.-S. Park, B. A. Remington, J. S. Ross, R. Tommasini, R. P. J. Town, V. Smalyuk, S. H. Glenzer, and E. I. Moses. Radiative shocks produced from spherical cryogenic implosions at the national ignition facility. *Physics of Plasmas*, 20(5):056315, 2013.

[6] T. Ditmire, E. Springate, J. W. G. Tisch, Y. L. Shao, M. B. Mason, N. Hay, J. P. Marangos, and M. H. R. Hutchinson. Explosion of atomic clusters heated by high-intensity femtosecond laser pulses. *Phys. Rev. A*, 57:369–382, Jan 1998.

[7] T. Ditmire, R. A. Smith, J. W. G. Tisch, and M. H. R. Hutchinson. High intensity laser absorption by gases of atomic clusters. *Phys. Rev. Lett.*, 78:3121–3124, Apr 1997.

[8] M. Hohenberger, D. R. Symes, J. Lazarus, H. W. Doyle, R. E. Carley, A. S. Moore, E. T. Gumbrell, M. M. Notley, R. J. Clarke, M. Dunne, and R. A. Smith. Observation of a velocity domain cooling instability in a radiative shock. *Phys. Rev. Lett.*, 105:205003, Nov 2010.

[9] J Osterhoff, D R Symes, A D Edens, A S Moore, E Hellewell, and T Ditmire. Radiative shell thinning in intense laser-driven blast waves. *New Journal of Physics*, 11(2):023022, 2009.

[10] Zel'Dovich and Raizer. *Physics of Shock Waves and High-Temperature Hydrodynamic Phenomena*. Dover, 2001.

[11] R.W.P. McWhirter and R.H. Huddlestone. *Plasma Diagnostic Techniques*. Academic Press, 1965.

[12] G. Cristoforetti, A. De Giacomo, M. Dell'Aglio, S. Legnaioli, E. Tognoni, V. Palleschi, and N. Omenetto. Local thermodynamic equilibrium in laser-induced breakdown spectroscopy: Beyond the mcwhirter criterion. *Spectrochimica Acta Part B: Atomic Spectroscopy*, 65(1):86 – 95, 2010.

[13] D. R. Bates, A. E. Kingston, and R. W. P. McWhirter. Recombination between electrons and

atomic ions. i. optically thin plasmas. *Proceedings of the Royal Society of London. Series A. Mathematical and Physical Sciences*, 267(1330):297–312, 1962.

[14] M. M. Marinak, G. D. Kerbel, N. A. Gentile, O. Jones, D. Munro, S. Pollaine, T. R. Dittrich, and S. W. Haan. Three-dimensional hydra simulations of national ignition facility targets. *Physics of Plasmas*, 8(5):2275–2280, 2001.

[15] J. J. MacFarlane, I. E. Golovkin, and P. R. Woodruff. Helios-cr – a 1-d radiation-magnetohydrodynamics code with inline atomic kinetics modeling. Technical report, Prism, 2010.

[16] Jon T. Larsen and Stephen M. Lane. Hyades—a plasma hydrodynamics code for dense plasma studies. *Journal of Quantitative Spectroscopy and Radiative Transfer*, 51(1–2):179 – 186, 1994. Special Issue Radiative Properties of Hot Dense Matter.

[17] W.M. Haynes. *CRC Handbook of Chemistry and Physics*.